Clinical Cancer Research

# Mechanisms and Antitumor Activity of a Binary EGFR/DNA–Targeting Strategy Overcomes Resistance of Glioblastoma Stem Cells to Temozolomide

Zeinab Sharifi[1,2], Bassam Abdulkarim[2,3], Brian Meehan[2], Janusz Rak[2,4], Paul Daniel[2,3], Julie Schmitt[2,5], Nidia Lauzon[2], Kolja Eppert[2,4], Heather M. Duncan[1,2], Kevin Petrecca[6], Marie-Christine Guiot[2,7], Bertrand Jean-Claude[2,5], and Siham Sabri[2,7]

## Abstract

**Purpose:** Glioblastoma (GBM) is a fatal primary malignant brain tumor. GBM stem cells (GSC) contribute to resistance to the DNA-damaging chemotherapy, temozolomide. The epidermal growth factor receptor (EGFR) displays genomic alterations enabling DNA repair mechanisms in half of GBMs. We aimed to investigate EGFR/DNA combi-targeting in GBM.

**Experimental Design:** ZR2002 is a "combi-molecule" designed to inflict DNA damage through its chlorethyl moiety and induce irreversible EGFR tyrosine kinase inhibition. We assessed its *in vitro* efficacy in temozolomide-resistant patient-derived GSCs, mesenchymal temozolomide-sensitive and resistant *in vivo*–derived GSC sublines, and U87/EGFR isogenic cell lines stably expressing EGFR/wild-type or variant III (EGFRvIII). We evaluated its antitumor activity in mice harboring orthotopic EGFRvIII or mesenchymal TMZ-resistant GSC tumors.

**Results:** ZR2002 induced submicromolar antiproliferative effects and inhibited neurosphere formation of all GSCs with marginal effects on normal human astrocytes. ZR2002 inhibited EGF-induced autophosphorylation of EGFR, downstream Erk1/2 phosphorylation, increased DNA strand breaks, and induced activation of wild-type p53; the latter was required for its cytotoxicity through p53-dependent mechanism. ZR2002 induced similar effects on U87/EGFR cell lines and its oral administration significantly increased survival in an orthotopic EGFRvIII mouse model. ZR2002 improved survival of mice harboring intracranial mesenchymal temozolomide-resistant GSC line, decreased EGFR, Erk1/2, and AKT phosphorylation and was detected in tumor brain tissue by MALDI imaging mass spectrometry.

**Conclusions:** These findings provide the molecular basis of binary EGFR/DNA targeting and uncover the oral bioavailability, blood–brain barrier permeability, and antitumor activity of ZR2002 supporting potential evaluation of this first-in-class drug in recurrent GBM.

## Introduction

Glioblastoma (GBM), a grade 4 astrocytoma, is the most common and aggressive malignant primary brain tumors in adults (1). The standard treatment of patients newly diagnosed with GBM implementing surgical tumor resection, chemoradiation using the DNA alkylating agent temozolomide followed by adjuvant temozolomide (Stupp-regimen) improved the median survival to 14.6 months (2). Tumor recurrence is inevitable, poses major challenges for clinical management, and leads to a fatal outcome. Several mechanisms account for GBM recurrence including activity of the O6-methylguanine-DNA methyltransferase (MGMT), which repairs cytotoxic DNA lesions such as, temozolomide-induced O6-methylguanine adducts (3). Chemo- and radioresistance of a small population of self-renewing, tumorigenic cancer stem cells termed tumor-initiating cells or glioma stem cells (GSC; ref. 4) prompted the need for effective molecularly targeted therapies (5). The epidermal growth factor receptor (EGFR), a key oncogene driver of chemo- and radioresistance displays gene alterations in more than half of primary GBMs (6). Activation of EGFR by ligand binding (e.g., EGF) triggers a cascade of cellular signaling events associated with increased cell proliferation and survival through downstream effectors including PI3-K/Akt, Ras–Raf—MAPK, and protein kinase C signaling pathways. The most common *EGFR* mutation, EGFRvIII (EGFR type III, de2-7, Δ EGFR; ref. 7) results in a ligand-independent and constitutively active receptor. EGFR and EGFRvIII confer protective effects in response to DNA-damaging agents through several mechanisms including increased repair of DNA strand breaks (DSB; ref. 8). Likewise, alterations of the tumor suppressor *TP53* pathway in 30% of patients newly diagnosed with GBM (9) affect DNA repair,

[1]Division of Experimental Medicine, McGill University, Montreal, Quebec, Canada. [2]Research Institute of McGill University Health Centre, Montreal, Quebec, Canada. [3]Department of Oncology, McGill University, Montreal, Quebec, Canada. [4]Department of Pediatrics, McGill University, Montreal, Quebec, Canada. [5]Department of Medicine, McGill University, Montreal, Quebec, Canada. [6]Department of Neurology and Neurosurgery, McGill University, Montreal, Quebec, Canada. [7]Department of Pathology, McGill University, Montreal, Quebec, Canada.

**Note:** Supplementary data for this article are available at Clinical Cancer Research Online (http://clincancerres.aacrjournals.org/).

**Corresponding Author:** Siham Sabri, Department of Pathology, McGill University and Research Institute of McGill University Health Centre, 1001 Decarie Blvd, Montreal, Quebec H4A 3J1, Canada. Phone: 514-934-1934, ext. 44686; Fax: 514-934-8392; E-mail: siham.sabri@mcgill.ca

Clin Cancer Res 2019;25:7594–608

**doi:** 10.1158/1078-0432.CCR-19-0955

## Translational Relevance

Glioblastoma (GBM), the most advanced and frequent brain tumor in adults, remains incurable. To overcome challenges in GBM treatment, we evaluated the potency of ZR2002, a first-in-class type II combi-molecule designed to irreversibly block EGFR signaling and damage DNA as an intact structure. We show that ZR2002 induces submicromolar cytotoxic activity against GBM stem cells (GSCs) resistant to temozolomide, the first-line chemotherapy for GBM and gefitinib, a clinical EGFR inhibitor. ZR2002 was well-tolerated orally and significantly increased survival in the aggressive U87/EGFRvIII and temozolomide-resistant mesenchymal GSC intracranial mouse models. Furthermore, mass spectrometry imaging provided the first evidence of its ability to cross the blood–brain barrier. Mechanistically, ZR2002 induced high levels of DNA damage with concomitant inhibition of EGFR-mediated MAPK/ERK and PI3K/AKT signaling pathways. On the basis of these findings, our group is committed to pursue the development of ZR2002 toward phase I clinical trial for patients with recurrent malignant gliomas.

cell-cycle progression, apoptosis, and senescence in response to various stress stimuli through transcriptional activation of multiple target genes, including $p21^{WAF1/CIP1}$ (p21; ref. 10).

The EGFR pathway can be disrupted by EGFR tyrosine kinase inhibitors (TKI), such as ZD1839 (Iressa, gefitinib) an orally active, selective EGFR-TKI that blocks signal transduction pathways involved in cancer cell proliferation and survival (11). However, treatment with adjuvant gefitinib did not significantly improve progression-free survival or overall survival in patients newly diagnosed with GBM (12).

In this study, we anticipate that the combinatorial approach termed "combi-targeting" seeking to design a "combi-molecule" as a single agent with two mechanisms of action could be applied. The "combi-targeting" concept has evolved since the inception of "type I combi-molecules" requiring hydrolytic cleavage to exert their dual mechanism of action toward type II combi-molecules, which do not require hydrolytic cleavage to exert their dual mechanism of action (13). Although the combi-targeting strategy has been described for breast (14), lung (15), and prostate cancers, its use for GBM had scant attention (16). Our group has characterized the dual EGFR/DNA targeting property of ZR2002 (6-(2-chloroethylamino)-4-anilinoquinazolines), a type II molecular prototype in breast cancer cell lines, wherein ZR2002 exerts its DNA-damaging function through its chlorethyl moiety with concomitant irreversible inhibition of EGFR-mediated proliferation, survival, and DNA repair mechanisms (14). We hypothesized that these properties in addition to its structure (Supplementary Fig. S1; ref. 14) as a relatively lipophilic small molecule might increase the prospects for crossing the blood–brain barrier (BBB) and overcoming the activation of intrinsic or adaptive DNA repair pathways involved in chemo- and radioresistance of GSCs (4). Given the central role of GSCs in tumor initiation, chemo- and radioresistance, and tumor relapse (17), we used patient-derived GSC neurosphere cultures to investigate the effects of ZR2002. Herein, we report the mechanism of action and the *in vivo* efficacy of a combi-molecule designed to possess mixed EGFR-TK inhibitory and DNA-damaging properties for the first time in GSCs and U87MG GBM cell lines isogenic for EGFR and EGFRvIII. We show that ZR2002 drastically suppressed GSC neurosphere growth in all GSC lines tested including a highly aggressive mesenchymal temozolomide-resistant GSC line. ZR2002 induced cytotoxic effects in U87MG isogenic GBM cell lines stably expressing EGFR or EGFRvIII within a submicromolar range. Mechanistically, ZR2002-induced cellular effects were associated with decreased phosphorylation of EGFR, Erk1/2-induced signaling, increased DNA damage and activation of wild-type (wt)p53. Importantly, we showed that oral administration of ZR2002 significantly increased survival in U87/EGFRvIII and the temozolomide-resistant GSC orthotopic xenografts mice models. In the latter, we further provide the proof-of-concept for ZR2002 delivery across the blood brain barrier BBB by MALDI imaging mass spectrometry (MALDI IMS) and its *in vivo* efficacy through decreased EGFR, Erk1/2, and AKT phosphorylation strongly supporting the potential clinical benefit of such combi-molecule in GBM.

## Materials and Methods

### Cell culture, drug treatment, and transfection

GSCs OPK111, OPK49, OPK161, 48EF, and OPK257 GSC lines (isolated from patients newly diagnosed with GBM, provided by Dr. K. Petrecca) were characterized by our group (18). Temozolomide-sensitive (1123IC12S) and temozolomide-resistant mesenchymal *in vivo*–derived GSCs sublines (1123IC7R and 1123IC8R) were established in the laboratory of Dr. J. Rak (19). Low passage number GSCs were maintained in NeuroCult NS-A Basal Medium (STEMCELL Technologies) with NeuroCult NS-A proliferation supplements (18). U87MG and its isogenic counterparts stably transfected to overexpress EGFR (U87/EGFRwt) or EGFRvIII (U87/EGFRvIII) GBM cell lines (provided by Dr. B. Jean-Claude; ref. 16) and normal human primary astrocytes (NHA) (provided by Dr. J. Rak) were maintained in DMEM supplemented with 10% FBS and incubated in 5% $CO_2$ atmosphere at 37°C. Supplementary Table S1 summarizes some molecular and genomic characteristics of GBM cell lines and GSCs used in this study. Cells were treated with DMSO (control), gefitinib/Iressa (Ark Pharm), temozolomide (Tocris), or ZR2002 (designed and synthesized in the laboratory of Dr. B. Jean-Claude, Supplementary Fig. S1) at the indicated doses. PLKO.1 shp53 vector (Addgene No.19119) was used to generate p53 knockdown of OPK49 GSC line. Cells were tested for *Mycoplasma* using the MycoAlert Kit (Lonza).

### GSCs growth assays and neurosphere formation assay

GSC neurosphere cultures were dissociated with Accumax (Millipore), then seeded in triplicate at 1,500 cells per 96-well for 24 hours before treatment with temozolomide, gefitinib, ZR2002, or DMSO for 5 days. Cell viability was assessed using the AlamarBlue assay (Invitrogen) according to the manufacturer's instructions. Drug sensitivity was also assessed using the neurosphere assay. Cells were seeded overnight, treated the next day with temozolomide, gefitinib, ZR2002, or DMSO, and the number of spheres over 50 μm in size was counted 14 to 20 days later (18).

### EGF-induced autophosphorylation assay and Western blot analysis

GSCs were seeded in NeuroCult (STEMCELL) medium overnight. U87/EGFR isogenic cell lines were allowed to attach

overnight, then serum-starved for 24 hours. U87/EGFR isogenic cell lines or GSCs were exposed to the drugs for 2 hours rinsed with PBS, treated with EGF (50 ng/mL) for 20 minutes, then rinsed with ice-cold PBS to stop treatment before lysing. For immunoblotting analysis, cells were seeded overnight in standard medium, treated (drug or control) for 48 hours at the indicated concentrations, washed twice (established cell lines) or collected (GSCs) with ice-cold PBS, then lysed with RIPA buffer (Boston BioProducts) supplemented with 0.2 mmol/L sodium orthovanadate, protease (Sigma-Aldrich) and phosphatase (Roche Diagnostics) inhibitors cocktails. Western blotting analysis on tumors excised from orthotopic mice xenografts was performed following brain tumor tissue homogenization, lysates preparation and analysis of the protein concentration, as described above. Proteins (30 μg, Pierce BCA Protein Assay Kit, Thermo Fisher Scientific Inc.) were electrophoretically separated in 12% SDS-PAGE and transferred onto PVDF membranes. Membranes were probed for phosphorylated EGFR (p-EGFR/Tyr1068), total EGFR, phospho-p44/42 MAPK (p-Erk1/2), total Erk1/2, p-Akt/Ser473, $p21^{WAF1/CIP1}$, p-histone-H2A.X (Ser139) (20E3), Caspase-3 (Cell signaling), PARP-1 (46D11) total Akt1/2/3 (H-136), p53 (DO-1, mutant (mut) and wild-type forms) (Santa Cruz) and β-actin (Sigma-Aldrich). Appropriate horseradish peroxidase–conjugated secondary antibodies (Life technologies) and chemiluminescence detection were used (Amersham, GE Healthcare). Quantification of Western blotting data normalized to corresponding total antibodies and controls was performed using ImageJ software.

### Alkaline comet assay

Cells were seeded, allowed to attach for 24 hours, treated with DMSO, temozolomide or ZR2002 (0, 1, 5, 10, 20, 50, or 100 μmol/L) for 2 hours. Cells were harvested, washed twice in PBS, and electrophoresed at 20 V, 400 mA for 20 minutes. Membranes were then, processed for staining with SYBR Gold (Molecular Probes). Comets (at least 50) were visualized at ×400 magnification and DNA damage was quantified using Comet Assay IV software to calculate tail moments, as described previously (15).

### MTT cell proliferation assay

NHAs and U87/EGFR isogenic cell lines (1,000–1,500 cells) were plated in triplicate in 96-well plates and allowed to adhere overnight. Cell viability and proliferation was measured following 5 days of treatment with indicated concentrations of each drug or DMSO using Vybrant MTT Cell Proliferation Assay Kit (Thermo Fisher Scientific) following the manufacturer's protocol. Absorbance at a wavelength of 570 nm was measured on a microplate reader (Bio-Rad).

### Clonogenic assay

Cells were plated in 6-well plates, allowed to adhere overnight, and treated with ZR2002 or DMSO at varying concentrations in standard medium for 2 hours. The medium was replaced with drug-free medium and cells were incubated for additional 8 to 14 days or until colonies (more than 50 cells) were formed. Cells were then fixed with 10% formalin and stained using 1.5% methylene blue to count colonies. The surviving fraction was normalized to the plating efficiency of the corresponding controls (18, 20).

### Dose-finding study and intracranial U87/EGFRvIII-Luc2 and 1123IC7R-Luc xenografts

Experiments were performed in accordance with a protocol approved by our Institutional Animal Care Committee (McGill University Health Centre Research Institute and McGill University, Montreal, Canada). We performed a dose-finding study evaluated in two schedules. In schedule No. 1 (Supplementary Fig. S3A), eight female nude mice received ZR2002 (100, 150, and 200 mg/kg/day) or control via oral (*per os* gavage ($n = 2$/treatment group). In this schedule, mice were treated every day for 5 days with ZR2002 or vehicle control. After the first treatment cycle, mice were given a 5-day break and the second 5-day treatment cycle was started. The following parameters and endpoints were evaluated for a total of 60 days from the start of the study: mortality, changes in body weights, skin toxicity, biochemistry assessment of blood levels of liver enzymes [alanine aminotransferase (ALT) and aspartate aminotransferase (AST)] and complete blood count (CBC). In schedule No. 2 (Supplementary Fig. S3A), 6 female nude mice received ZR2002 ($n = 3$) or control ($n = 3$; 150 mg/kg, orally) for 21 consecutive days. The following parameters and endpoints were evaluated for 60 days: mortality, changes in body weights, skin toxicity, and CBC.

For Kaplan–Meier survival studies, U87/EGFRvIII and 1123IC7R GSC line were lentivirally transduced with a luciferase-BFP dual gene vector (Luc2 pSMALB; Luc2 cloned from pGL4.51 (Promega) into the pSMALB backbone described previously; ref. 21) to monitor tumor growth using bioluminescence imaging (BLI). For orthotopic injection, cells were dissociated to single-cell suspensions, and 20,000 cells were stereotactically injected into brains of 6- to 8-week-old nude mice (Charles River). Three days after U87/EGFRvIII-Luc2 cells implantation, mice were anesthetized with isoflurane and subsequently administered 15 μg/mL of D-luciferin [D-luciferin potassium salt (Cedarlane)] via intraperitoneal injection to perform BLI for pretreatment time point. For mice injected with U87/EGFRvIII cell line, mice were randomized into vehicle (control; $n = 7$) or ZR2002 150 mg/kg, orally ($n = 6$). For mice injected with 1123IC7R GSC line, mice were randomized into vehicle (control; $n = 6$) or temozolomide/66 mg/kg ($n = 6$) or gefitinib/150 mg/kg ($n = 6$) or ZR2002/150 mg/kg ($n = 6$) given orally. Tumor growth was monitored by BLI (19) using an IVIS 200 scanner (PerkinElmer).

For intracranial tumor models, body weights were recorded and mice were sacrificed upon significant weight loss (>20%) or presentation of neurologic symptoms necessitating euthanasia. Mice brains were collected following perfusion with formalin for Western blotting analysis on orthotopic tumors xenografts and for IHC analysis of brain tissue sections. Tumors were excised for brain tumor tissue homogenization followed by lysing for Western blotting analysis and for paraffin embedding. Paraffin blocks were processed in 4-μm thick sections for automated Ki-67 IHC staining on BenchMark XT (Ventana Medical Systems). Slides were digitally scanned using an Aperio scanner scope XT and positively stained nuclei were quantified using ImageJ by two independent observers.

### MALDI imaging mass spectrometry

MALDI imaging mass spectrometry (MALDI IMS) was performed on tissue sections (Supplementary Methods) on a MALDI TOF/TOF Ultraflextreme mass spectrometer equipped with a SmartBeam II Nd:YAG 355 nm laser (Bruker Daltonics).

### Statistical analysis

Data are reported as mean ± SD and are representative of at least 3 independent experiments run in triplicate, unless otherwise stated. Statistics were performed using unpaired two-tailed Student *t* test. A Kaplan–Meier survival test was used for survival studies in mice. Analysis was performed using GraphPad Prism (GraphPad Software Inc.). *P* values <0.05 were considered statistically significant.

## Results

### Antiproliferative effects of ZR2002 in GSCs

We first investigated the effect of ZR2002 in a panel of patient-derived primary GSCs (OPK111, OPK49, OPK161, 48EF, and OPK257), which exhibit different EGFR expression levels, as shown by immunoblotting analysis (Fig. 1A). ZR2002 reduced the viability (AlamarBlue) of OPK111, OPK49, OPK161, 48EF, and OPK257 at the $IC_{50}$ concentrations of 0.69, 0.60, 0.50, 0.39, and 1.77 μmol/L, respectively (Fig. 1B; Supplementary Table S2). Of note, ZR2002 is highly effective against MGMT-positive GSCs (48EF, OPK111, and OPK161) and MGMT-negative (OPK257 and OPK49), previously characterized by our group (18) for their MGMT expression levels (Supplementary Table S1). Interestingly, all GSC neurosphere cultures were highly resistant to temozolomide ($IC_{50}$ >100 μmol/L) and displayed $IC_{50}$ concentrations ranging between 24 and 55 μmol/L in response to gefitinib treatment.

We subsequently verified the effects of ZR2002 on mesenchymal temozolomide-sensitive GSC (1123IC12S) and temozolomide-resistant variant GSC lines (1123IC7R and 1123IC8R) previously derived from NOD SCID gamma (NSG) immunodeficient mice harboring intracranial tumors of the parental GSC line (1123ICP, mutp53 R248L) and treated *in vivo* with temozolomide (19). 1123IC7R mutp53 R248L GSCs lacks a functional DNA mismatch repair (MMR) pathway, as it has gained MMR deficiency during temozolomide treatment (MSH4: G21R mutation and MLH3: E506K mutation and decreased expression of two MMR genes, MSH2 and MSH6, Supplementary Table S1). As expected (19), 1123IC12S was sensitive to temozolomide ($IC_{50}$: ∼21 μmol/L), whereas 1123IC7R and 1123IC8R (MMR-deficient, MGMT-negative) were resistant to temozolomide ($IC_{50}$: >100 μmol/L).

Strikingly, our results revealed that 1123IC12S, 1123IC7R, and 1123IC8R were highly sensitive to ZR2002, reaching $IC_{50}$'s in the submicromolar range (∼0.6 μmol/L) regardless of their sensitivity to temozolomide (Fig. 1C). To ascertain whether ZR2002 antiproliferative effects might affect normal brain cells, we used MTT proliferation assay to investigate its effects on NHA. ZR2002 exhibited at least 10-fold higher $IC_{50}$ for NHA compared with GSCs (∼12 μmol/L; Fig. 1D), suggesting that its antiproliferative effects on GSCs may not affect noncancer cells. Collectively, our data demonstrate that ZR2002 had striking antiproliferative effects on GSCs derived from patients newly diagnosed with GBM, a mesenchymal temozolomide-sensitive and resistant GSC lines, but not on NHA.

### Inhibition of EGFR-induced downstream signaling, neurosphere formation, and increased DSBs in GSCs

We have previously shown that ZR2002 induced irreversible inhibition of EGF-stimulated autophosphorylation in breast cancer cell lines (14). Western blot analysis showed that ZR2002 treatment of GSCs at 1 μmol/L (Fig. 2A and B) was sufficient to attenuate EGFR tyrosine phosphorylation (Tyr1068) and to dramatically reduce Erk1/2 and Akt phosphorylation (Ser473), thereby blocking downstream signaling pathways in all tested GSC lines with varied levels of EGFR and MGMT expression. Interestingly, gefitinib induced similar effects at the $IC_{50}$ 20 μmol/L (lowest range for gefitinib $IC_{50}$s in GSCs), while temozolomide did not show any effects at a concentration as high as 100 μmol/L.

We further performed a time course experiment to assess phosphorylation of γ-H2AX at Ser139, a hallmark of DSBs induced by DNA damage. Western blotting analysis showed that ZR2002 (1 μmol/L, 2 hours) induced a slight increase in the levels of p-γ-H2AX in 1123IC12S mesenchymal GSCs (Fig. 2C) while upregulation of p-γ-H2AX in 1123IC7R GSCs was detected only after 24 hours following ZR2002 treatment. The upregulation of p-γ-H2AX in both mesenchymal GSCs tested was sustained up to the last time point tested (48 hours).

Congruent results were also obtained with the neurosphere assay for OPK111, OPK49, 48EF and OPK161 GSCs, which failed to form neurospheres following 1 μmol/L ZR2002 treatment compared with DMSO control, while gefitinib (20 μmol/L) only partially affected neurosphere formation and temozolomide had no effect at 100 μmol/L (Fig. 3A and B). We subsequently tested the DNA-damaging potential of ZR2002 GSCs using the comet assay. ZR2002 treatment (1 μmol/L, 2 hours) resulted in significantly higher levels of DNA damage in GSCs compared with DMSO control (Fig. 3C, $P < 0.0001$). As expected, treatment with temozolomide for 2 hours induced barely detectable levels of DNA damage at concentrations as high as 100 μmol/L. Figure 3D shows representative images of DNA comets in 48EF treated with ZR2002 (1 μmol/L) or temozolomide (100 μmol/L).

### Antiproliferative effects of ZR2002 are associated with inhibition of EGFR autophosphorylation and its DNA-damaging effects in U87/EGFR isogenic cell lines

To determine whether ZR2002 exhibits cytotoxicity for cells with EGFR overexpression (EGFRwt) or expressing the constitutively active variant EGFRvIII, we used GBM U87/EGFR isogenic cell lines. Immunoblotting analysis confirmed that U87MG cells had low EGFR expression levels while U87/EGFR isogenic cell lines had high expression of EGFRwt (U87/EGFRwt) or EGFRvIII (U87/EGFRvIII; Fig. 4A).

We used MTT viability/proliferation assay to assess the cytotoxicity of ZR2002 and determine the $IC_{50}$ of ZR2002, temozolomide, gefitinib, or DMSO control in U87/EGFR isogenic cell lines. ZR2002 treatment reduced cell viability in a dose-dependent manner and exhibited strikingly low $IC_{50}$s for U87MG, U87/EGFRwt and U87/EGFRvIII (0.78, 0.76 and 0.6 μmol/L, respectively) (Fig. 4B). Importantly, ZR2002 displayed approximately 27, 23, and 41-fold superior antiproliferative activity over gefitinib in U87MG, U87/EGFRwt, and U87/EGFRvIII cells, respectively. Temozolomide up to 100 μmol/L did not decrease the viability of these cell lines, as previously reported (22).

To further explore the cytotoxic effects induced by ZR2002, we performed a clonogenic assay to analyze the colony formation ability of U87/EGFR isogenic cells. ZR2002 at 1 μmol/L (short exposure for 2 hours then growth in drug-free medium for 8–14 days) reduced the clonogenic survival of all EGFR/isogenic cell lines tested (Supplementary Fig. S2). U87/EGFRvIII cells were significantly more sensitive to ZR2002 at 5 μmol/L compared with U87MG ($P = 0.0013$) and U87/EGFRwt ($P = 0.0156$). The plating

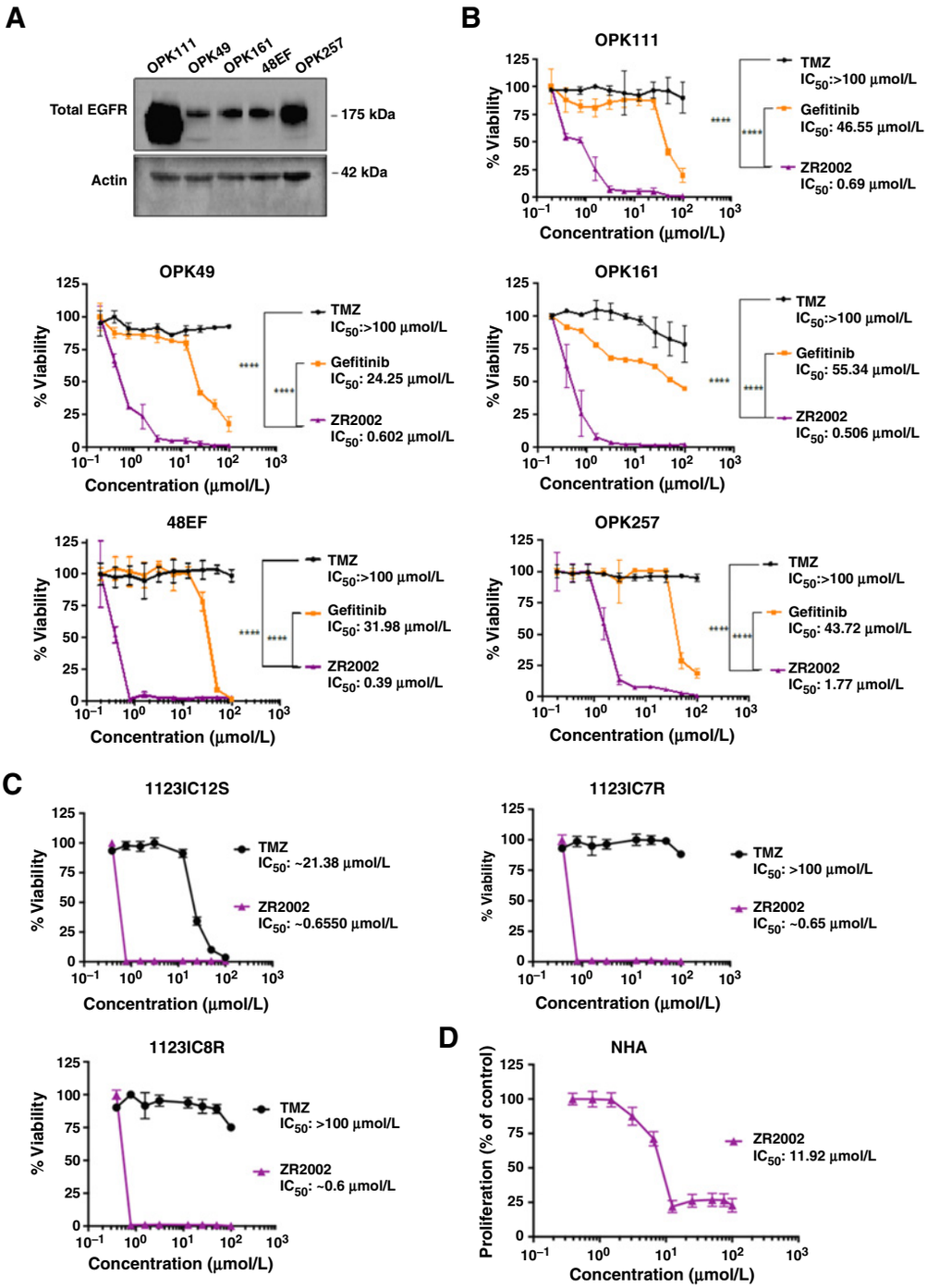


**Figure 1.**

**A–D,** ZR2002 significantly inhibits proliferation of GSCs at doses that do not affect proliferation of NHA. **A,** Western blotting analysis of EGFR expression levels in a panel of 5 patient-derived primary GSCs ($n = 3$). Actin was used as a loading control. **B,** GSCs were treated with various concentrations of DMSO, temozolomide (TMZ), gefitinib, or ZR2002 for 5 days and cell proliferation was measured using Alamar blue assay (****, $P < 0.0001$). **C,** Effect of ZR2002 compared with temozolomide treatment of temozolomide-sensitive (1123IC12S) and temozolomide-resistant (1123IC7R and 1123IC8R) GSCs was measured using Alamar blue assay (5-day treatment). **D,** NHAs were treated with ZR2002 at various concentrations for 5 days, and cell proliferation was measured using MTT assay. Graphs represent mean values ± SD from at least three independent experiments in triplicate.

efficiencies of U87MG, U87/EGFRwt, and U87/EGFRvIII cells at 5 μmol/L ZR2002 (mean ± SD) were 0.1 ± 5, 0.11 ± 10, and 0.06 ± 4.3, respectively (Supplementary Fig. S2A). Supplementary Figure S2B shows a representative image of the drastic effects of ZR2002 (5 μmol/L) on U87/EGFRvIII compared with DMSO control.

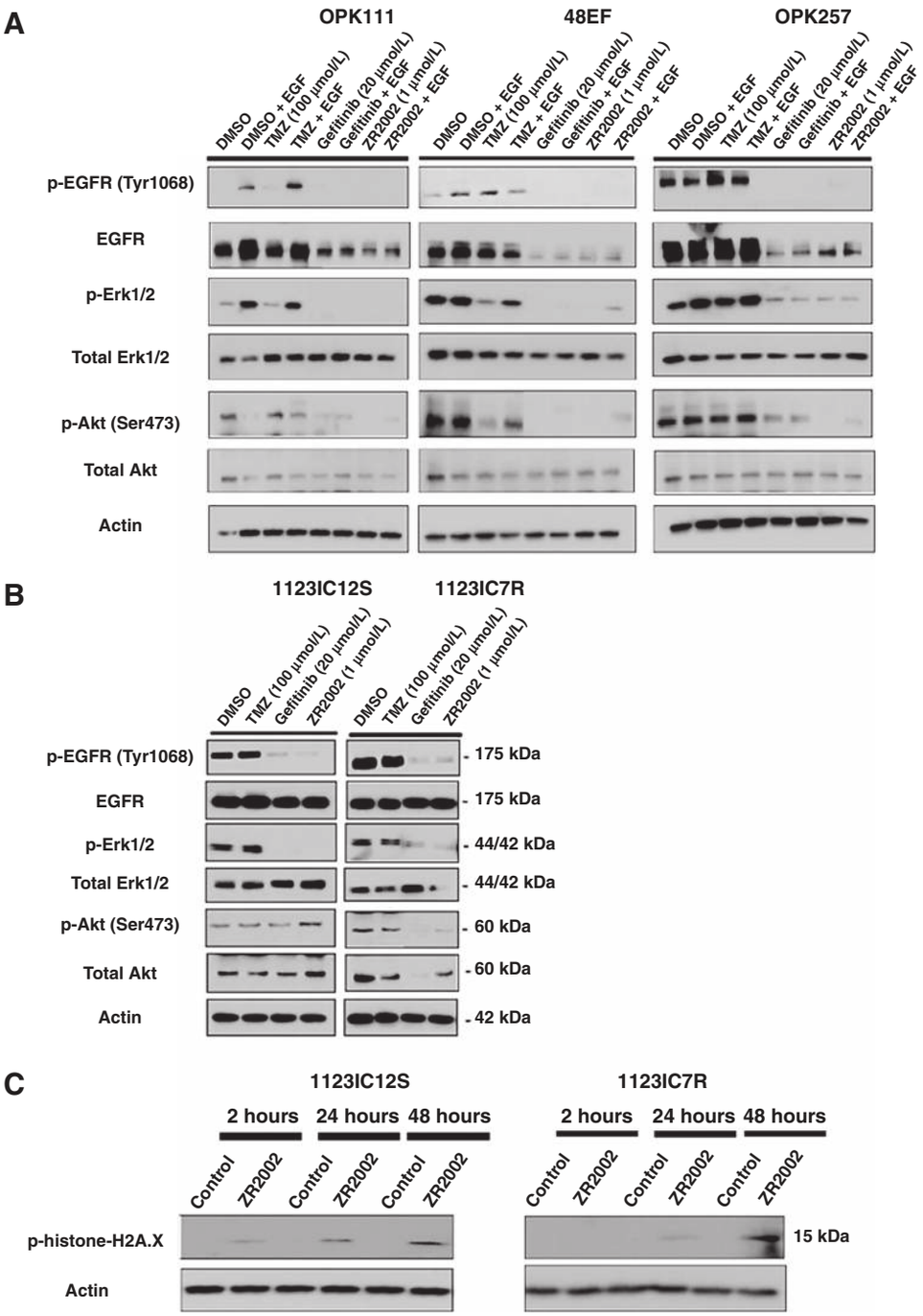


**Figure 2.**

**A–C,** ZR2002 inhibits EGFR-induced downstream signaling and increased γ-H2AX in mesenchymal (1123IC12S and 1123IC7R) GSCs. OPK111, 48EF and OPK257 (**A**), 1123IC12S and 1123IC7R GSCs (**B**) were treated with temozolomide (TMZ; 100 μmol/L), gefitinib (20 μmol/L), ZR2002 (1 μmol/L), or DMSO control for 2 hours, stimulated or not with EGF (50 ng/mL) for 20 minutes, then probed for p-EGFR (Tyr1068), total EGFR, p-Erk1/2, total Erk1/2, p-Akt (Ser473), total Akt, and actin as a loading control by Western blotting ($n = 2$). **C,** 1123IC12S and 1123IC7R were treated with 1 μmol/L ZR2002 for 2, 24, and 48 hours and then lysed and probed for p-histone-H2AX (Ser 139) and actin as a loading control by Western blotting.

We investigated the ability of ZR2002 to inhibit EGFR autophosphorylation in U87/EGFR isogenic cell lines (Fig. 4C). Cells were treated with temozolomide (100 μmol/L), gefitinib (20 μmol/L), or ZR2002 (1 μmol/L) with or without EGF (2 hours) and the effects on EGFR autophosphorylation (Tyr1068) and downstream signaling were analyzed by Western blotting. ZR2002 treatment (only 1 μmol/L, 2 hours) induced complete inhibition of EGF-induced EGFR autophosphorylation), and downregulated Erk1/2 phosphorylation, which may account for its antiproliferative effects in EGFR-expressing isogenic cell lines (Fig. 4C).

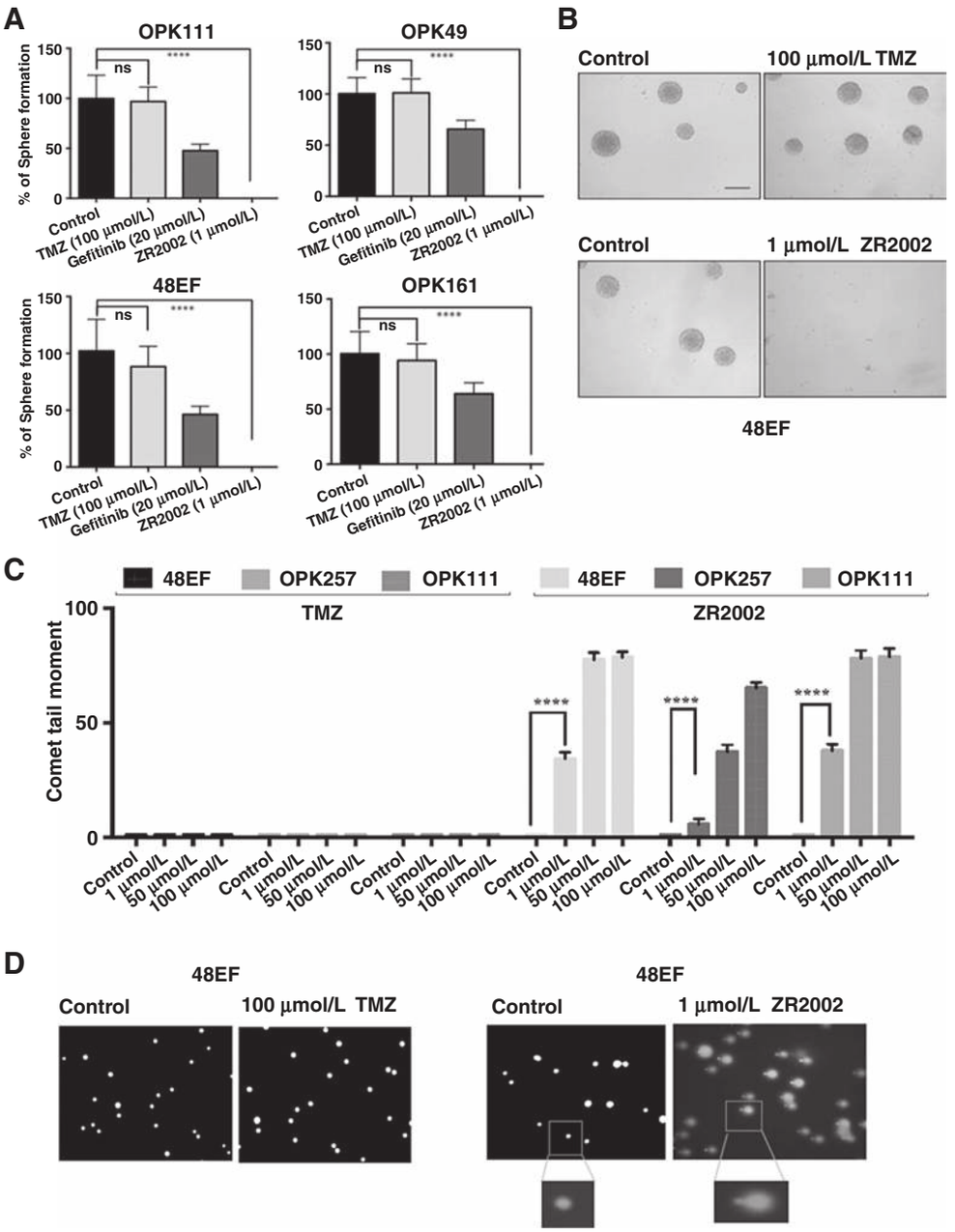


**Figure 3.**

**A–D,** ZR2002 inhibits neurosphere formation ability of GSCs and inflicts DNA damage in GSCs. **A,** Sphere formation results for GSCs after treatment with temozolomide (TMZ; 100 μmol/L), gefitinib (20 μmol/L), ZR2002 (1 μmol/L), or DMSO control. Ten random fields were photographed for both vehicle and drug-treated conditions and the number of spheres over 50 μm in size was scored 14 to 20 days later from three independent experiments in duplicate. **B,** Representative images of 48EF treated with temozolomide (100 μmol/L) or ZR2002 (1 μmol/L). Scale bar, 200 μm. **C,** Cells were exposed to ZR2002 or temozolomide for 2 hours and assessed for drug-induced DNA damage using an alkaline comet assay. Average comet tail moments were calculated from 50 comets based on three independent experiments for each concentration. **D,** Representative images of DNA comets stained with SYBR Gold dye and visualized by fluorescence microscopy are shown for ZR2002 (1 μmol/L) and compared with temozolomide (100 μmol/L) in 48EF (****, $P < 0.0001$; ns, not significant).

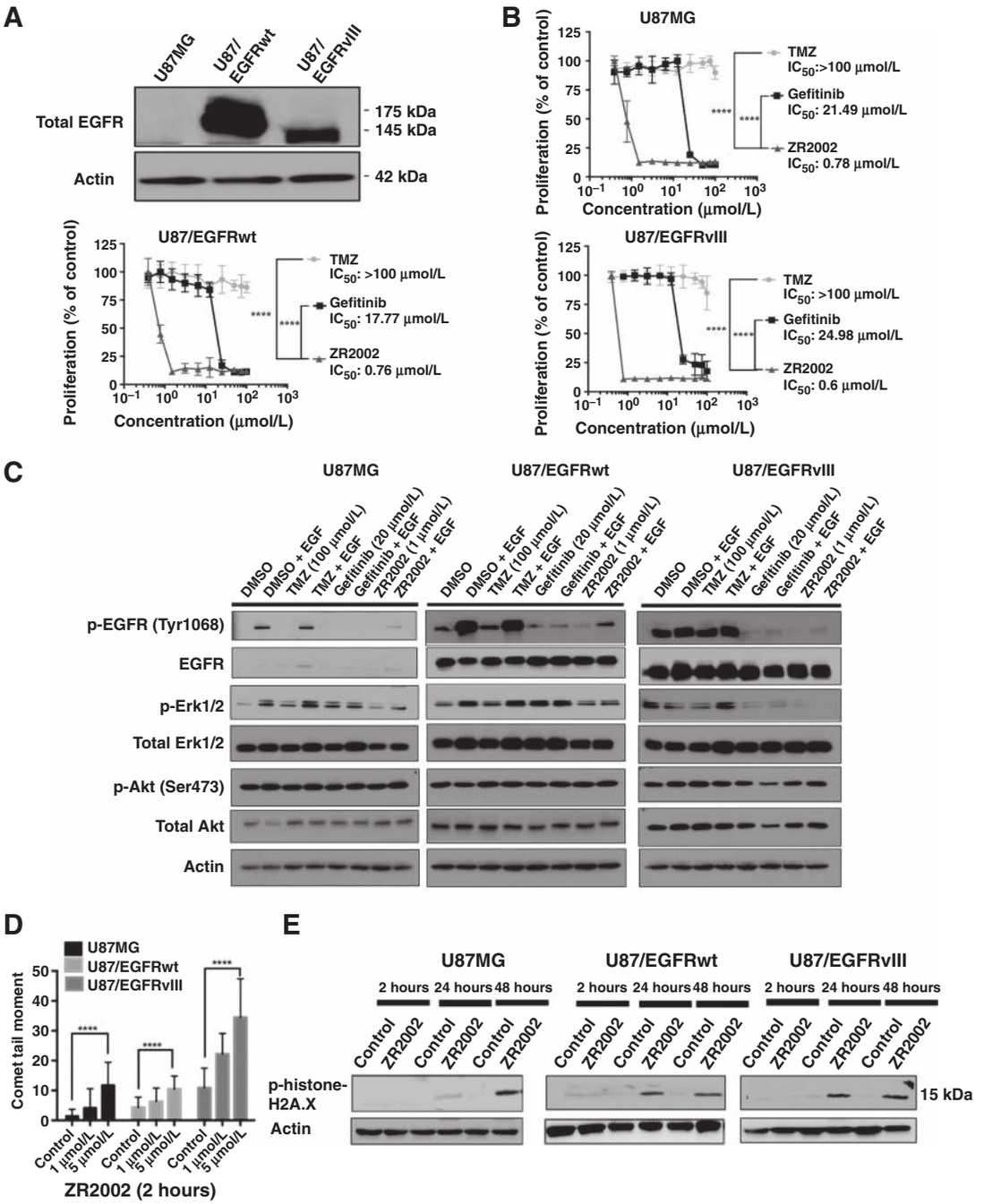


**Figure 4.**

**A–E,** Antiproliferative effects of ZR2002 are associated with inhibition of EGFR autophosphorylation, its DNA-damaging effects in U87/EGFR isogenic cell lines. **A,** Western blotting analysis of EGFR levels in U87/EGFR isogenic lines ($n = 2$). **B,** Cells were treated with various concentrations of DMSO, temozolomide (TMZ), gefitinib, or ZR2002 for 5 days. Cell proliferation was measured using Vybrant MTT Cell Proliferation Assay Kit. Graphs represent mean values ± SD from at least three independent experiments in triplicate ****, $P < 0.0001$. **C,** Serum-starved U87MG, U87/EGFRwt and U87/EGFRvIII cells were treated with temozolomide (100 μmol/L), gefitinib (20 μmol/L), ZR2002 (1 μmol/L), or DMSO control for 2 hours, stimulated or not with EGF (50 ng/mL), lysed, then probed by Western blotting ($n = 2$) for p-EGFR (Tyr1068), total EGFR, p-Erk1/2, total Erk1/2, p-Akt (Ser473), total Akt, and actin as a loading control. **D,** Cells were exposed to for 2 hours and assessed for drug-induced DNA damage using an alkaline comet assay. Average tail moments were calculated from 50 comets based on three independent experiments for each concentration ($P$ value for each condition compared with DMSO control is shown, ****, $P < 0.0001$). **E,** U87/EGFR isogenic cell lines were treated with 1 μmol/L ZR2002 for 2, 24, and 48 hours and then lysed and probed for p-histone-H2AX (Ser 139) and actin as a loading control by Western blotting.

Increasing exposure time showed expression of P-EGFR, its inhibition by ZR2002 in U87MG and oversaturation of chemiluminescence signal in EGFR-overexpressing cell lines (Supplementary Fig. S2C). As expected, ZR2002 did not affect Akt phosphorylation (Ser473) of U87/EGFR isogenic cell lines due to their PTEN-deficient status (23).

We subsequently tested the DNA-damaging potential of ZR2002 on U87/EGFR isogenic cell lines using the comet assay. ZR2002 at an early time point (5 μmol/L, for only 2 hours) significantly increased the levels of DNA strand breakage in single cells as reflected by comet tails analysis in all U87 isogenic cell lines compared with their respective controls ($P < 0.0001$; Fig. 4D). Supplementary Figure S2D shows dose-dependent increase number of comet tails following treatment with concentrations up to 100 μmol/L for all U87 isogenic cell lines with noticeable effects seen for U87/EGFRvIII compared to its isogenic counterparts. As expected, temozolomide treatment did not significantly increase DNA damage in these cells (data not shown).

Compared with its respective DMSO control, ZR2002 treatment (1 μmol/L) increased phosphorylation of γ-H2AX at 48 hours in U87MG cell line and induced comparable kinetics of increased phosphorylation of γ-H2AX at 24- and 48-hour time points in U87/EGFRwt and U87/EGFRvIII cell lines (Fig. 4E). ZR2002 treatment decreased pro-caspase-3 expression levels, but cleaved caspase-3 fragment was barely detectable in U87/EGFRwt and U87/EGFRvIII cell lines (data not shown).

### ZR2002 mechanism of action is mediated through wtp53 activation

Upon DNA damage, ataxia-telangiectasia (ATM), Rad3-related (ATR), and DNA-PK activate p53 through phosphorylation (24). Treatment with temozolomide (100 μmol/L), or ZR2002 (1 μmol/L), or gefitinib (20 μmol/L) induced a marked increase in p53 levels and was accompanied by induction of its known target p21 protein in U87/isogenic cell lines (wt*TP53*) and OPK161, OPK49, 48EF, OPK257, and OPK111 (wt*TP53*) with the exception of OPK257 (mut*TP53*; Fig. 5A and B; ref. 18). To further explore the effect of p53 inhibition on ZR2002 treatment, we used OPK49 GSC line, which showed the greatest increase of p53 protein expression levels upon exposure to ZR2002 (Fig. 5B) and performed shRNA-mediated *TP53* knockdown. We achieved at least 90% decrease of p53 expression with concomitant decrease of expression levels of p53 target protein, p21 (Fig. 5C). Next, we examined whether p53-knockdown affects the growth inhibitory effects of ZR2002. Silencing of p53 caused a significant increase in drug resistance in OPK49/shRNA ($P < 0.0001$; $IC_{50}$:0.66 and 2.66 μmol/L in OPK49 and OPK49/shRNA, respectively; Fig. 5D). To further explore the effect of p53 status on sensitivity to ZR2002 in OPK49, we performed a neurosphere formation assay. OPK49/shRNA was able to form neurospheres, despite treatment with ZR2002 at 1 μmol/L, whereas the same concentration completely inhibited neurosphere formation of OPK49 mock cell line (Fig. 5E).

### ZR2002 is well tolerated, crosses the BBB, and improves survival of mice with EGFRvIII and 1123IC7R intracranial tumors

To assess the *in vivo* efficacy of ZR2002, we performed a dose-finding study to evaluate the optimal dose of ZR2002 in nude mice. In schedule No. 1 (Supplementary Fig. S3A) mice were treated (oral gavage of 100, 150 and 200mg/kg/day of ZR2002 or vehicle control) every day for 5 days, followed by a 5-day break then a second 5-day cycle, then monitored up to 60 days post-treatment. ZR2002 at doses up to 150 mg/kg was well tolerated. Mice were alive without having weight loss >20% (Supplementary Fig. S3B), did not show any significant changes in CBC, liver enzymes ALT/AST (Supplementary Tables S3) or skin toxicity, which could be a concern, as previously reported for EGFR inhibitors (25). We monitored toxicity in mice treated with 150 mg/kg ZR2002 (orally) for 21 consecutive days (schedule No. 2, Supplementary Fig. S3A). Over an observation period of 60 days post-treatment, ZR2002 (150 mg/kg) did not show any significant difference compared to vehicle control groups for mortality, weight loss (Supplementary Fig. S3C), skin toxicity, or CBC counts (Supplementary Table S4).

Next, we assessed the *in vivo* efficacy of ZR2002 in a mouse orthotopic U87/EGFRvIII GBM xenograft model known for their high rate of intracranial tumor growth and short median survival (26). U87/EGFRvIII-Luc2 cells were stereotactically injected into the striatum of nude mice only 4 days before starting treatment. After the second 5-day treatment cycle, 4 of 7 mice in the control group showed significant weight loss (>20%), while none of the mice in the ZR2002 group showed significant weight loss (>20%; Fig. 6A). ZR2002 significantly reduced tumor BLI signal compared to control group at the same time point ($P = 0.0262$) (Fig. 6B). Interestingly, ZR2002 at 150 mg/kg significantly improved survival of mice compared to the control group ($P = 0.0003$; Fig. 6C; Supplementary Fig. S4A). Hence, ZR2002 exhibits antiproliferative effects within a submicromolar range *in vitro* and anti-tumor activity in the highly aggressive U87/EGFRvIII orthotopic model without toxicity in nude mice.

We also assessed the *in vivo* efficacy of ZR2002 in the highly aggressive intracranial xenograft 1123IC7R GSC mesenchymal temozolomide-resistant mouse model (19). Three days following stereotactic injection of 1123IC7R GSCs stably transfected with luciferase (1123IC7R-luc), mice were treated once daily with either vehicle control (3 weeks), temozolomide (66 mg/kg, 5 days; ref. 27), gefitinib (150 mg/kg, 3 weeks; ref. 28), or ZR2002 (150 mg/kg, 3 weeks) and monitored for tumor growth using BLI imaging. Figure 6D shows representative images of BLI signals from mice in control and treatment groups at different time points. Remarkably, ZR2002 treatment significantly prolonged the survival of mice compared with vehicle control ($P = 0.005$; Fig. 6E; Supplementary Fig. S4B).

Mice were given a final dose of 150 mg/kg (ZR2002 or gefitinib) and 66 mg/kg temozolomide prior to euthanasia to assess downstream signaling effectors on tumor tissue by Western blotting. ZR2002 dramatically reduced EGFR, Erk1/2, and AKT phosphorylation in 1123IC7R (Fig. 6F).

In accordance with previous studies showing that GSCs exhibit pronounced apoptotic resistance (29), we did not detect cleaved caspase-3 fragment by Western blotting in 1123IC7R tumor lysates *in vivo*, neither following ZR2002 treatment of 1123IC7R GSCs in time course experiments *in vitro*, wherein pro-caspase-3 was decreased at 48-hour time point (data not shown). To further investigate the onset of ZR2002-induced cell death, we used Western blotting to analyze expression and apoptotic and/or necrotic processing of PARP-1, a key enzyme involved in DNA repair in response to strand breaks in addition to DNA damage–

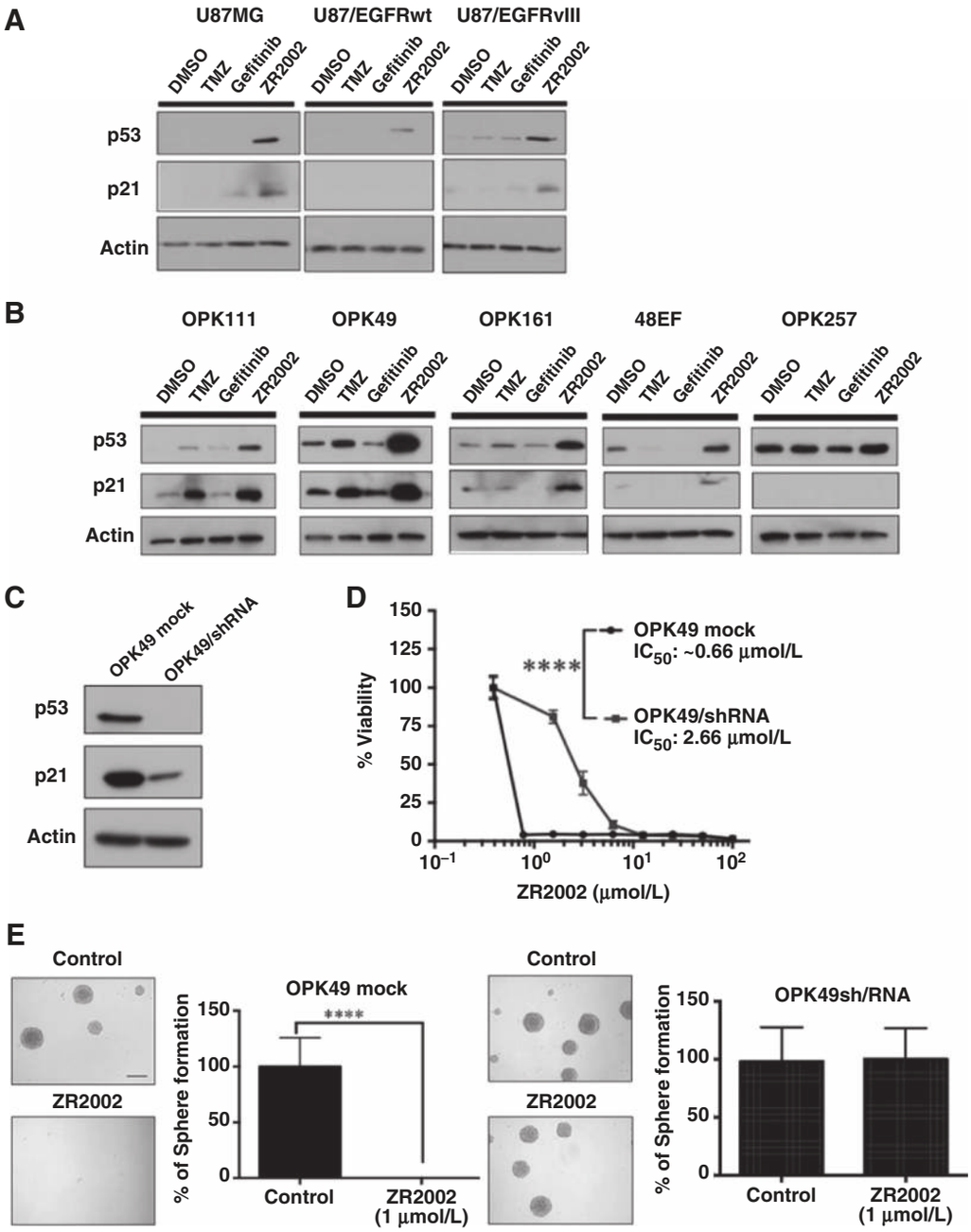


**Figure 5.**

**A–E,** ZR2002 mechanism of action is mediated through wtp53 activation. **A** and **B,** Western blotting analysis showing p53 and p21 expression in GBM-established cell lines (**A**) and GSCs (**B**) treated for 48 hours with DMSO, temozolomide (TMZ; 100 μmol/L), gefitinib (20 μmol/L), or ZR2002 (1 μmol/L). Cell lysates were probed with p53 antibody, then reprobed for p21 and actin as a loading control. **C,** Western blotting confirmed p53-knockdown by at least 95% in OPK49/shp53. **D** and **E,** p53-knockdown induced resistance to ZR2002 compared with the parental OPK49, as shown in viability assay (**D**; graph represent mean values ± SD from at least three independent experiments in triplicate) and sphere formation assay (**E**; from three independent experiments in duplicate; ****, $P < 0.0001$). Scale bar, 200 μm.

induced necrotic cell death following excessive DNA damage. Interestingly, treatment with ZR2002 increased expression of the full length of PARP-1 (116 kDa), while cleavage of the apoptotic fragment of 89 kDa was detectable and the major necrotic cleavage fragment of 50 kDa, previously reported as a hallmark of DNA-damage induced necrosis (30) was noticeable in 2 of 4 tumors analyzed (Fig. 6G).

ZR2002 significantly decreased numbers of cells that stained positive for the proliferative marker Ki-67, which is consistent with decreased phosphorylation of Erk1/2 shown by Western

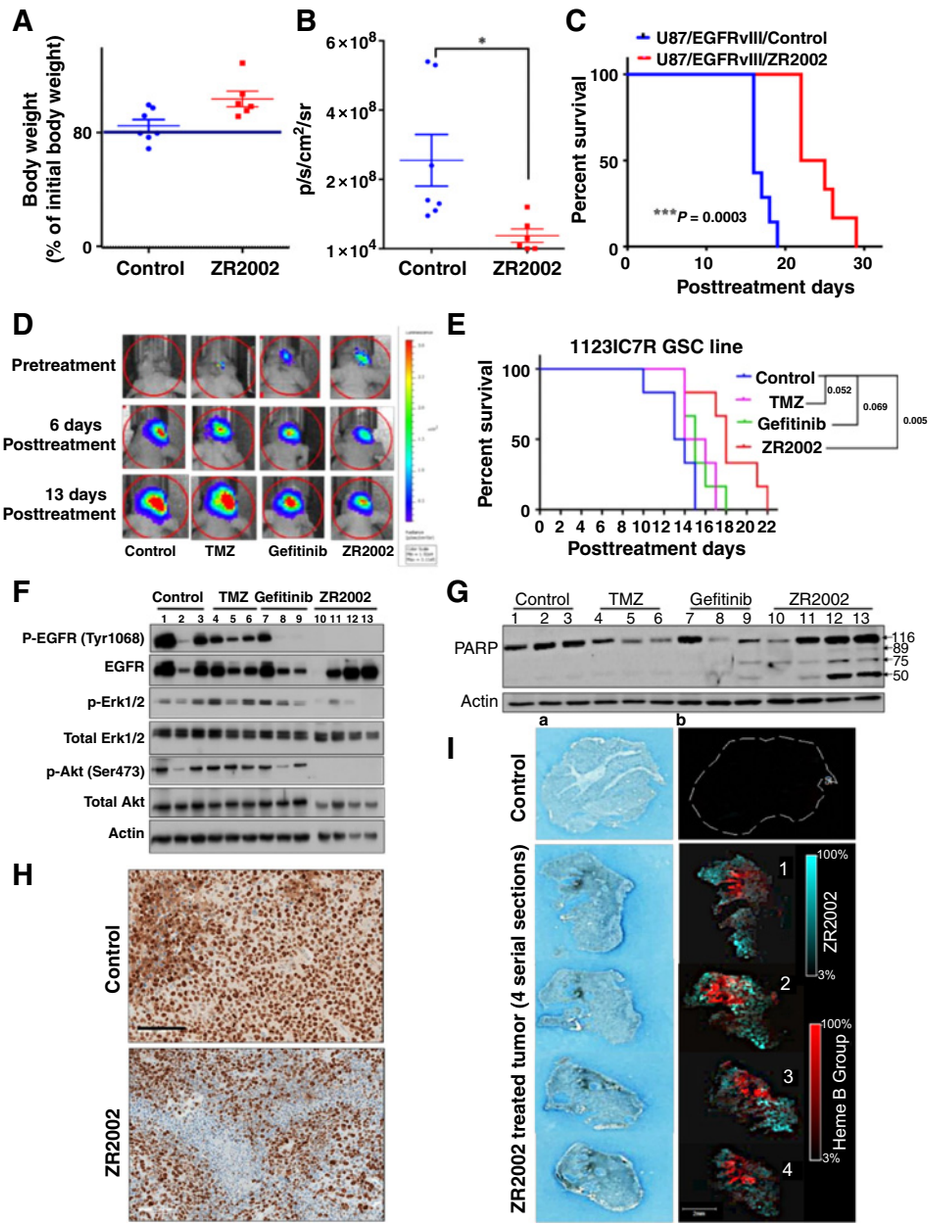


**Figure 6.**

**A–I,** ZR2002 is well tolerated, crosses the blood–brain barrier, and improves survival of mice with EGFRvIII and 1123IC7R intracranial tumors. **A,** U87/EGFRvIII-Luc2 was stereotactically injected into the brain of nude mice. After 4 days, mice were orally treated with vehicle control ($n = 7$) or ZR2002 150 mg/kg ($n = 6$) according to schedule No. 1. Body weights of mice are shown for the end of the second 5-day treatment cycle. **B,** BLI signal of mice is shown for the same time point (end of the second 5-days cycle; *statistical significance for control vs. ZR2002, $P = 0.0262$). **C,** Survival curves were generated for EGFRvIII-Luc2 intracranial tumors; ***, $P = 0.0003$. **D** and **E,** 1123IC7R-Luc2 GSCs were stereotactically injected into the brain of nude mice. After 3 days, mice were orally treated with vehicle control ($n = 6$) temozolomide (TMZ)/66 mg/kg ($n = 6$), gefitinib/150 mg/kg ($n = 6$), or ZR2002/150 mg/kg ($n = 6$) according to schedule No. 2. **D,** Tumor growth was monitored using BLI and representative images of BLI signal are shown at pretreatment, 6 days and 13 days posttreatment for each treatment group. **E,** Kaplan–Meier survival curves were generated for 1123IC7R-Luc2 GSC intracranial tumors; *statistical significance ($P = 0.005$); ns, not significant (control vs. temozolomide; $P = 0.0529$), (control vs. gefitinib; $P = 0.069$). **F** and **G,** Mice were given a final dose of control, ZR2002, gefitinib, or temozolomide before euthanasia. Tumor tissue collected from mice brains was processed for lysis (**F** and **G**) to analyze by Western blotting p-EGFR (Tyr1068), total EGFR, p-Erk1/2, total Erk1/2, p-Akt (Ser473), total Akt, PARP-1, and actin, and also paraffin embedding for IHC staining (**H**) as shown in representative images of Ki-67 IHC staining for control and ZR2002 conditions. Scale bar, 100 μm **I,** MALDI IMS for blood brain barrier permeability of ZR2002. **a,** Optical scan of tissue after CHCA deposition revealed the brain margin on four serial brain sections. **b,** Distribution of ZR2002 is shown in the mouse brain treated with ZR2002 (turquoise, *m/z*377.01) and absent in the control. Heme (red, *m/z*616.18) served as a marker for the lumen of blood vessels. Scale bar, 2 mm.

blotting (Fig. 6F). Supplementary Figure S6 shows Ki-67 IHC scoring analysis comparing ZR2002 treatment with vehicle control ($P < 0.0001$). Figure 6H shows representative images of decreased Ki-67 proliferative index, which also revealed patterns of ZR2002-induced necrotic cell death in areas with less cellular density. This is in line with the presence of the necrotic cleavage fragment of 50 kDa in the corresponding brain 1123IC7R tumor tissue analyzed by Western blotting (last lane, Fig. 6G).

Interestingly, MALDI IMS (31) provided the perspective to assess brain tumor permeability of ZR2002 through the BBB in an intracranial 1123IC7R mouse model (Fig. 6I). Isotopic pattern and MS/MS ($m/z377.0 \rightarrow m/z341.0$) were used to confirm the presence of ZR2002 on-tissue (Supplementary Fig. S5). Hematoxylin and eosin (H&E) staining confirmed the presence of tumor (Supplementary Fig. S7A). Optical scan of tissue after CHCA deposition revealed the brain margin on four serial brain sections (Fig. 6I, panel a). Distribution of ZR2002 is shown in the mouse brain treated with ZR2002 (turquoise signal), while absent in a mouse treated with vehicle control (Fig. 6I, panel b). Heme (red, $m/z616.18$) was used as a marker for the lumen of blood vessels (31, 32). IMS potentially detected ZR2002 dealkylated metabolite (ZR01; ref. 14, $m/z315.0$), a potent EGFR inhibitor in the brain of treated mouse (Supplementary Fig. S7B and S7C). As expected, both signals of ZR2002 and ZR01 are co-localized on the treated tissue and absent from the control (overlay of ZR2002 and ZR01 signals in yellow, Supplementary Fig. S7D). Taken together, our data indicate that ZR2002 is well-tolerated in nude mice, crosses the BBB and improves survival of mice with EGFRvIII or 1123IC7R intracranial tumors.

## Discussion

Despite compelling evidence demonstrating the potential of EGFR as a target in GBM, EGFR-targeted agents did not fulfill their promise in the treatment of patients newly diagnosed with GBM (12) or with recurrent disease (33). In this study, we present novel findings for the potential clinical efficacy of ZR2002, a small molecule designed to block EGFR-mediated signaling but in contrast to other EGFR inhibitors, it carries a haloalkyl arm capable of reacting with the receptor itself and with DNA bases, and importantly was kept small enough to maintain brain penetrability. First, we provide experimental evidence for a unique growth inhibitory profile of ZR2002 in experimental settings that recapitulates the heterogeneity and aggressive nature of GBM disease. This includes (i) MGMT-positive or negative GSCs derived from newly diagnosed GBM patients; (ii) an experimental GSC model for *in vivo* temozolomide resistance and GBM recurrence with the highly aggressive temozolomide-resistant mesenchymal *in vivo* derived MMR-deficient GSC subline; and (iii) GBM established cell lines isogenic for EGFR or EGFRvIII. Second, our study highlights the cytotoxic effects of ZR2002 through DNA damage (DSBs) shown by comet assay with concomitant inhibition of EGFR or EGFRvIII-induced downstream signaling. Importantly, its DNA damaging arm seems to act in a p53-dependent manner, as suggested by increased expression of p53 in all GSCs (except for mutantp53 OPK257) and the causal relationship between *TP53* activation and the antiproliferative effects of ZR2002 in wtp53 GSC line. Third, we achieved a key step in pre-clinical development of ZR2002 and showed its safety, BBB permeability, oral bioavailability and *in vivo* anti-tumor properties with significant delay of tumor progression for either EGFRvIII-driven or mesenchymal GSC temozolomide-resistant intracranial xenografts in nude mice. Thus, our results suggest DNA damage with concomitant irreversible inhibition of EGFR tyrosine kinase activity as a key vulnerability in GBM. The concept of EGFR oncogene "addiction" has gained a momentum based on clinical evidence for the success of different EGFR-targeted therapies in different cancer types. Further experimental evidence revealed the role of EGFR as a key oncogene driver at the nexus of tumor metabolism and immunogenic cell death (34). Oncogenic TKs orchestrate complex signaling pathways, cross-talk with each other, trigger similar signaling pathways that enable alternate compensatory mechanisms following inhibition with RTK inhibitor as a monotherapy. The potency of ZR2002 stems from its conceptual design to achieve divergent targeting of different cellular components (i.e, co-targeting a RTK and DNA) (14, 16). Our findings showing the *in vivo* potency of ZR2002 support the concept of divergent targeting as an efficient and promising multi-targeting approach beyond co-targeting RTKs to inhibit downstream compensatory mechanisms.

Given the important role of GSCs as a disease reservoir in GBM, unraveling the molecular mechanisms involved in the maintenance of GSCs provided the rationale for preclinical and clinical testing of targeted therapeutic strategies aiming to eradicate GSCs (5). ZR2002 displayed cytotoxic antiproliferative effects with an $IC_{50}$ within a submicromolar range and drastically obliterated neurosphere formation of GSCs including MGMT-positive GSCs intrinsically resistant to temozolomide (48EF, OPK111 and OPK161) and MGMT-negative MMR-deficient GSC line (1123IC7R, Supplementary Table S1). Our results are in accordance with studies showing that EGFR-knockdown in EGFR-positive GBM neurosphere cultures led to differentiation and less malignant tumors *in vivo*, and its inhibition resulted in reduced neurosphere formation in the presence of EGF (35).

Our study provides some mechanistic insights underlying the antiproliferative effects and potency of ZR2002 to eradicate neurosphere forming ability and improve survival in a highly aggressive GSC model refractory to temozolomide and gefitinib. Tyr1068, has been reported as one major EGFR autophosphorylation site (36), which is key in Ras–Raf–MAPK ERK1/2 pathway (37). Our *in vitro* and *in vivo* experiments show that ZR2002 treatment drastically downregulated this tyrosine kinase site. It has been previously reported that temozolomide and ZR2002 are able to induce methylation of genomic DNA (22) and ZR2002 alkylating chloroethyl function (14), respectively. ZR2002 inflicts DNA damage inducing DNA strand breaks through its DNA-damaging moiety as shown by comet assay in breast cancer cell lines (14) and in the current study, in which ZR2002 induced sustained increased γ-H2AX phosphorylation reminiscent of persistence of DSBs and low efficiency of DNA repair (Fig. 2C and Fig. 4E). We surmise that its EGFR TK-targeting moiety irreversibly induces covalent damage to ATP site, which subsequently cutback EGFR-mediated DSB repair. Indeed, besides its canonical role as a cell surface receptor in signal transduction to downstream effectors, EGFR is shuttled to the nucleus (38). Several studies provided convincing evidence for the role of nuclear EGFR in transcriptional regulation (cyclin D1) (39), DNA

synthesis, and repair and showed its role in chemo- and radioresistance and association with worst clinical prognosis (40). Nuclear EGFR directly interacts with and enhances the activity of DNA-PKcs known for their major role in nonhomologous end joining of DSBs repair (41) in addition to its direct interaction with histone H4 affecting DNA synthesis and repair (42). Furthermore, a study by Yakoub and colleagues demonstrated that EGFR is also involved in upregulation of DNA repair genes such as XRCC1 and ERCC1 (43). Additional studies are needed to identify the specific mechanism(s) by which ZR2002 inhibits EGFR-mediated repair of DNA damage (decrease in DNA synthesis and repair in GBM), which might be critical for its *in vivo* efficacy.

Resistance to apoptosis in GBM (29, 44) is heightened with loss of a functional p53 response (45) and gain of MMR-deficiency during temozolomide treatment (46). Our orthotopic *in vivo* experiments revealed that ZR2002 induced drastic anti-proliferative effects (low Ki67 proliferation index and suppression of P-ERk1/2 induced signaling), while promoting to some extent necrotic cell death with evidence of PARP-1 necrotic cleavage and necrotic areas in brain tumor tissue of mutp53 MMR-deficient 1123IC7R GSC temozolomide-resistant mouse model. This is in line with the tenet that DNA damage triggers necrosis cell death as a self-determined cell fate through PARP-1 activation independently from p53, Bax/Bak, or caspases (47). Excessive DNA damage and/or DNA repair defects with overwhelming unrepaired DNA breaks lead to sustained PARP-1 activation, inhibition of glycolysis, depletion of cellular ATP pools, and necrotic cell death (48–50).

In accordance with the important role of p53 in response to DNA damage, ZR2002 treatment increased expression of wtp53 to a variable extent in EGFR isogenic cell lines and GSCs, and this increase was more pronounced compared to temozolomide or gefitinib. Accordingly, increased expression of its downstream effector p21, a readout of p53 activation known to mediate cell-cycle checkpoints and apoptosis (51) might support ZR2002-induced cytotoxicity. Previous work has shown that loss of functional p53 increased the sensitivity of normal and neoplastic astrocytic cells to DNA alkylating agents (52). Dinca and colleagues (53) demonstrated in an intracranial xenograft model that U87MG cells were sensitized to temozolomide by pretreatment with pifithrin-α (inhibitor of p53). Loss of functional p53 was previously shown to contribute to stemness and survival in GSCs (54). The relationship between p53 and sensitivity to ZR2002 in wtp53 GSC line (OPK49), wherein p53-silencing by RNAi significantly conferred resistance to ZR2002 (Fig. 6D), suggests that ZR2002 might partially exert its effects on GSCs in a p53-dependent manner and extends on previous findings corroborating the role of functional p53 in GSCs in response to DNA damage.

ZR2002 exhibited *in vitro* and *in vivo* effects on U87/EGFRvIII cell line unveiling EGFR/DNA binary targeting as a novel strategy to directly inhibit EGFRvIII. Thus far, strategies targeting EGFRvIII-positive GBM tumors has failed in GBM (55, 56). EGFRvIII has been shown to enhance DSB repair in a mouse orthotopic glioma model (57). Co-expression of EGFRvIII and PTEN (negative regulator of PI3K/Akt pathway) in GBM cells is associated with heightened sensitivity to EGFR kinase inhibitors, while PTEN deficiency decreases response to EGFR inhibitors due to high levels of Akt activation (58). Accordingly, ZR2002 induced marked dephosphorylation of EGFR and Erk1/2, but not p-Akt (Ser473) in PTEN-deficient (23) U87/EGFR isogenic cell lines.

Collectively, our findings demonstrate the drastic effects of ZR2002 on GSG neurosphere formation *in vitro* and its *in vivo* efficacy in a temozolomide -resistant GSC model in addition to noticeable cytotoxic effects on EGFRvIII *in vitro* and *in vivo*. Our study highlights binary EGFR/DNA–targeting strategy to induce irreversible inhibition of EGF-stimulated autophosphorylation, while increasing DSBs as a potentially attractive therapeutic strategy to overcome EGFR-induced compensatory DNA repair mechanisms in GBM. It also provides the proof-of-principle to suggest ZR2002 as a novel approach in GBM including for patients with recurrent temozolomide-resistant GBM, for which effective therapeutic options are not currently available.

## Disclosure of Potential Conflicts of Interest

No potential conflicts of interest were disclosed.

## Authors' Contributions

**Conception and design:** Z. Sharifi, B. Abdulkarim, J. Rak, B. Jean-Claude, S. Sabri

**Development of methodology:** Z. Sharifi, B. Abdulkarim, J. Rak, K. Eppert, M.-C. Guiot, B. Jean-Claude, S. Sabri

**Acquisition of data (provided animals, acquired and managed patients, provided facilities, etc.):** Z. Sharifi, B. Meehan, J. Rak, P. Daniel, N. Lauzon, K. Petrecca, S. Sabri

**Analysis and interpretation of data (e.g., statistical analysis, biostatistics, computational analysis):** Z. Sharifi, B. Abdulkarim, B. Meehan, N. Lauzon, K. Petrecca, M.-C. Guiot, B. Jean-Claude, S. Sabri

**Writing, review, and/or revision of the manuscript:** Z. Sharifi, B. Abdulkarim, P. Daniel, J. Schmitt, N. Lauzon, H.M. Duncan, K. Petrecca, B. Jean-Claude, S. Sabri

**Administrative, technical, or material support (i.e., reporting or organizing data, constructing databases):** Z. Sharifi, B. Abdulkarim, K. Eppert, S. Sabri

**Study supervision:** B. Abdulkarim, S. Sabri

**Other (synthesis of ZR2002):** J. Schmitt

**Other (development of materials):** H.M. Duncan

**Other (pathology review and IHC development and scoring):** M.-C. Guiot

## Acknowledgments

This study was supported by the Canadian Cancer Society Research Institute-Innovation grant No. 702178 (to S. Sabri), Cancer Research Society Operating grant No. 22716 (to S. Sabri), Montreal General Hospital Foundation (salary support including Simone & Morris Fast Award), and McGill University Health Centre Foundation (to S. Sabri). This work was partially supported by a donation from Susan Aberman and Louis Dzialowski through The Montreal Neurological Hospital Foundation (to B. Abdulkarim and S. Sabri). The authors thank the Drug Discovery Platform, Histopathology Platform, and Glen Animal Facility of the Research Institute of McGill University Health Centre (RI-MUHC) for their valuable technical support and expertise.

The costs of publication of this article were defrayed in part by the payment of page charges. This article must therefore be hereby marked *advertisement* in accordance with 18 U.S.C. Section 1734 solely to indicate this fact.

Received March 21, 2019; revised June 21, 2019; accepted September 18, 2019; published first September 20, 2019.

## References


1. Wen PY, Kesari S. Malignant gliomas in adults. N Engl J Med 2008;359: 492–507.
2. Stupp R, Mason WP, Van Den Bent MJ, Weller M, Fisher B, Taphoorn MJ, et al. Radiotherapy plus concomitant and adjuvant temozolomide for glioblastoma. N Engl J Med 2005;352:987–96.
3. Hegi ME, Diserens A-C, Gorlia T, Hamou M-F, de Tribolet N, Weller M, et al. MGMT gene silencing and benefit from temozolomide in glioblastoma. N Engl J Med 2005;352:997–1003.
4. Bao S, Wu Q, McLendon RE, Hao Y, Shi Q, Hjelmeland AB, et al. Glioma stem cells promote radioresistance by preferential activation of the DNA damage response. Nature 2006;444:756–60.
5. Osuka S, Van Meir EG. Overcoming therapeutic resistance in glioblastoma: the way forward. J Clin Invest 2017;127:415.
6. Eskilsson E, Røsland GV, Solecki G, Wang Q, Harter PN, Graziani G, et al. EGFR heterogeneity and implications for therapeutic intervention in glioblastoma. Neuro-oncol 2018;20:743–52.
7. Gan HK, Cvrljevic AN, Johns TG. The epidermal growth factor receptor variant III (EGFRvIII): where wild things are altered. FEBS J 2013;280: 5350–70.
8. Liccardi G, Hartley JA, Hochhauser D. EGFR nuclear translocation modulates DNA repair following cisplatin and ionizing radiation treatment. Cancer Res 2011;71:1103–14.
9. England B, Huang T, Karsy M. Current understanding of the role and targeting of tumor suppressor p53 in glioblastoma multiforme. Tumour Biol 2013;34:2063–74.
10. Bai L, Zhu W-G. p53: structure, function and therapeutic applications. J Cancer Mol 2006;2:141–53.
11. Vivanco I, Robins HI, Rohle D, Campos C, Grommes C, Nghiemphu PL, et al. Differential sensitivity of glioma-versus lung cancer–specific EGFR mutations to EGFR kinase inhibitors. Cancer Discov 2012;2: 458–71.
12. Uhm JH, Ballman KV, Wu W, Giannini C, Krauss J, Buckner JC, et al. Phase II evaluation of gefitinib in patients with newly diagnosed Grade 4 astrocytoma: Mayo/North Central Cancer Treatment Group Study N0074. Int J Radiat Oncol Biol Phys 2011;80:347–53.
13. Qiu Q, Domarkas J, Banerjee R, Katsoulas A, McNamee JP, Jean-Claude BJ. Type II combi-molecules: design and binary targeting properties of the novel triazolinium-containing molecules JDD36 and JDE05. Anticancer Drugs 2007;18:171–7.
14. Brahimi F, Rachid Z, Qiu Q, McNamee JP, Li YJ, Tari AM, et al. Multiple mechanisms of action of ZR2002 in human breast cancer cells: a novel combimolecule designed to block signaling mediated by the ERB family of oncogenes and to damage genomic DNA. Int J Cancer 2004;112: 484–91.
15. Mouhri ZS, Goodfellow E, Jean-Claude B. A type I combi-targeting approach for the design of molecules with enhanced potency against BRCA1/2 mutant-and O6-methylguanine-DNA methyltransferase (mgmt)-expressing tumour cells. BMC Cancer 2017;17:540.
16. Watt HL, Rachid Z, Jean-Claude BJ. The concept of divergent targeting through the activation and inhibition of receptors as a novel chemotherapeutic strategy: signaling responses to strong DNA-reactive combinatorial mimicries. J Signal Transduct 2012;2012:282050.
17. Stiles CD, Rowitch DH. Glioma stem cells: a midterm exam. Neuron 2008; 58:832–46.
18. Patyka M, Sharifi Z, Petrecca K, Mansure J, Jean-Claude B, Sabri S. Sensitivity to PRIMA-1MET is associated with decreased MGMT in human glioblastoma cells and glioblastoma stem cells irrespective of p53 status. Oncotarget 2016;7:60245.
19. Garnier D, Meehan B, Kislinger T, Daniel P, Sinha A, Abdulkarim B, et al. Divergent evolution of temozolomide resistance in glioblastoma stem cells is reflected in extracellular vesicles and coupled with radiosensitization. Neuro-oncol 2017;20:236–48.
20. Valiathan C, McFaline JL, Samson LD. A rapid survival assay to measure drug-induced cytotoxicity and cell cycle effects. DNA Repair (Amst) 2012; 11:92–8.
21. van Galen P, Kreso A, Wienholds E, Laurenti E, Eppert K, Lechman ER, et al. Reduced lymphoid lineage priming promotes human hematopoietic stem cell expansion. Cell Stem Cell 2014;14:94–106.
22. Lee SY. Temozolomide resistance in glioblastoma multiforme. Genes Dis 2016;3:198–210.
23. Lee J, Kim B, Park M, Lee Y, Kim Y, Lee B, et al. PTEN status switches cell fate between premature senescence and apoptosis in glioma exposed to ionizing radiation. Cell Death Differ 2011;18:666.
24. Maréchal A, Zou L. DNA damage sensing by the ATM and ATR kinases. Cold Spring Harb Perspect Biol 2013;5:a012716.
25. Chanprapaph K, Vachiramon V, Rattanakaemakorn P. Epidermal growth factor receptor inhibitors: a review of cutaneous adverse events and management. Dermatol Res Pract 2014;2014:734249.
26. Yoshida Y, Ozawa T, Yao T-W, Shen W, Brown D, Parsa AT, et al. NT113, a pan-ERBB inhibitor with high brain penetrance, inhibits the growth of glioblastoma xenografts with EGFR amplification. Mol Cancer Ther 2014; 13:2919–29.
27. Carlson BL, Grogan PT, Mladek AC, Schroeder MA, Kitange GJ, Decker PA, et al. Radiosensitizing effects of TMZ observed *in vivo* only in a subset of MGMT methylated GBM xenografts. Int J Radiat Oncol Biol Phys 2009;75: 212.
28. Sharma J, Lv H, Gallo JM. Intratumoral modeling of gefitinib pharmacokinetics and pharmacodynamics in an orthotopic mouse model of glioblastoma. Cancer Res 2013;73:5242–52.
29. Valdés-Rives SA, Casique-Aguirre D, Germán-Castelán L, Velasco-Velázquez MA, González-Arenas A. Apoptotic signaling pathways in glioblastoma and therapeutic implications. BioMed Res Int 2017;2017:7403747.
30. Gobeil S, Boucher C, Nadeau D, Poirier G. Characterization of the necrotic cleavage of poly (ADP-ribose) polymerase (PARP-1): implication of lysosomal proteases. Cell Death Differ 2001;8:588.
31. Liu X, Ide JL, Norton I, Marchionni MA, Ebling MC, Wang LY, et al. Molecular imaging of drug transit through the blood-brain barrier with MALDI mass spectrometry imaging. Sci Rep 2013;3:2859.
32. Baijnath S, Naiker S, Shobo A, Moodley C, Adamson J, Ngcobo B, et al. Evidence for the presence of clofazimine and its distribution in the healthy mouse brain. J Mol Histol 2015;46:439–42.
33. Wen PY, Chang SM, Lamborn KR, Kuhn JG, Norden AD, Cloughesy TF, et al. Phase I/II study of erlotinib and temsirolimus for patients with recurrent malignant gliomas: North American Brain Tumor Consortium trial 04-02. Neuro-oncol 2014;16:567–78.
34. Perez R, Crombet T, de Leon J, Moreno E. A view on EGFR-targeted therapies from the oncogene-addiction perspective. Front Pharmacol 2013;4:53.
35. Howard BM, Gursel DB, Bleau A-M, Beyene RT, Holland EC, Boockvar JA. EGFR signaling is differentially activated in patient-derived glioblastoma stem cells. J Exp Ther Oncol 2009;8:247–60.
36. Downward J, Parker P, Waterfield M. Autophosphorylation sites on the epidermal growth factor receptor. Nature 1984;311:483.
37. Wee P, Wang Z. Epidermal growth factor receptor cell proliferation signaling pathways. Cancers 2017;9:52.
38. Lin S-Y, Makino K, Xia W, Matin A, Wen Y, Kwong KY, et al. Nuclear localization of EGF receptor and its potential new role as a transcription factor. Nat Cell Biol 2001;3:802.
39. Diehl JA. Cycling to cancer with cyclin D1. Cancer Biol Ther 2002;1: 226–31.
40. Lo H-W. Nuclear mode of the EGFR signaling network: biology, prognostic value, and therapeutic implications. Discov Med 2010;10:44.
41. Mukherjee B, Choy H, Nirodi C, Burma S. Targeting nonhomologous end-joining through epidermal growth factor receptor inhibition: rationale and strategies for radiosensitization. Semin Radiat Oncol 2010;20: 250–7.
42. Chou R-H, Wang Y-N, Hsieh Y-H, Li L-Y, Xia W, Chang W-C, et al. EGFR modulates DNA synthesis and repair through Tyr phosphorylation of histone H4. Dev Cell 2014;30:224–37.
43. Yacoub A, McKinstry R, Hinman D, Chung T, Dent P, Hagan MP. Epidermal growth factor and ionizing radiation up-regulate the DNA repair genes XRCC1 and ERCC1 in DU145 and LNCaP prostate carcinoma through MAPK signaling. Radiat Res 2003;159:439–52.
44. Mohammad RM, Muqbil I, Lowe L, Yedjou C, Hsu H-Y, Lin L-T, et al. Broad targeting of resistance to apoptosis in cancer. Semin Cancer Biol 2015; 35Suppl:S78–S103.

45. Shetzer Y, Solomon H, Koifman G, Molchadsky A, Horesh S, Rotter V. The paradigm of mutant p53-expressing cancer stem cells and drug resistance. Carcinogenesis 2014;35:1196–208.
46. Sarkaria JN, Kitange GJ, James CD, Plummer R, Calvert H, Weller M, et al. Mechanisms of chemoresistance to alkylating agents in malignant glioma. Clin Cancer Res 2008;14:2900–8.
47. Zong W-X, Ditsworth D, Bauer DE, Wang Z-Q, Thompson CB. Alkylating DNA damage stimulates a regulated form of necrotic cell death. Genes Dev 2004;18:1272–82.
48. Shin H-J, Kwon H-K, Lee J-H, Gui X, Achek A, Kim J-H, et al. Doxorubicin-induced necrosis is mediated by poly-(ADP-ribose) polymerase 1 (PARP1) but is independent of p53. Sci Rep 2015;5:15798.
49. Fouquerel E, Goellner EM, Yu Z, Gagne J-P, de Moura MB, Feinstein T, et al. ARTD1/PARP1 negatively regulates glycolysis by inhibiting hexokinase 1 independent of NAD+ depletion. Cell Rep 2014;8:1819–31.
50. Galluzzi L, Vitale I, Aaronson SA, Abrams JM, Adam D, Agostinis P, et al. Molecular mechanisms of cell death: recommendations of the Nomenclature Committee on Cell Death 2018. Cell Death Differ 2018; 25:486.
51. Chen J. The cell-cycle arrest and apoptotic functions of p53 in tumor initiation and progression. Cold Spring Harb Perspect Med 2016;6: a026104.
52. Xu GW, Nutt CL, Zlatescu MC, Keeney M, Chin-Yee I, Cairncross JG. Inactivation of p53 sensitizes U87MG glioma cells to 1, 3-bis (2-chloroethyl)-1-nitrosourea. Cancer Res 2001;61:4155–9.
53. Dinca EB, Lu KV, Sarkaria JN, Pieper RO, Prados MD, Haas-Kogan DA, et al. p53 Small-molecule inhibitor enhances temozolomide cytotoxic activity against intracranial glioblastoma xenografts. Cancer Res 2008;68: 10034–9.
54. Firat E, Niedermann G. FoxO proteins or loss of functional p53 maintain stemness of glioblastoma stem cells and survival after ionizing radiation plus PI3K/mTOR inhibition. Oncotarget 2016;7:54883.
55. Swartz AM, Li Q-J, Sampson JH. Rindopepimut: a promising immunotherapeutic for the treatment of glioblastoma multiforme. Immunotherapy 2014;6:679–90.
56. Malkki H. Trial Watch: Glioblastoma vaccine therapy disappointment in Phase III trial. Nat Rev Neurol 2016;12:190.
57. Mukherjee B, McEllin B, Camacho CV, Tomimatsu N, Sirasanagandala S, Nannepaga S, et al. EGFRvIII and DNA double-strand break repair: a molecular mechanism for radioresistance in glioblastoma. Cancer Res 2009;69:4252–9.
58. Mellinghoff IK, Wang MY, Vivanco I, Haas-Kogan DA, Zhu S, Dia EQ, et al. Molecular determinants of the response of glioblastomas to EGFR kinase inhibitors. N Engl J Med 2005;353:2012–24.